Electronic Supplementary Material (ESI) for Catalysis Science & Technology.

Electronic Supporting Information for:

Identifying the time-dependent predominance regimes of step and terrace sites for the Fischer-Tropsch synthesis on Ruthenium based catalysts

Dalia Liuzzi, Francisco J. Pérez-Alonso, F. Javier García-García, F. Calle-Vallejo, José Luis G. Fierro and Sergio Rojas

S1. Catalyst characterization

Powder X-ray diffraction (XRD) patterns were recorded in the 4 - 90º 2θ range in the scan mode (0.04 º, 20 s) using an X´Pert Pro PANalytical diffractometer. Figure S1 shows the X-ray diffraction patterns of all catalysts under study. The characteristic set of reflection lines for the rutile and anatase phases of the TiO_2 structure are clearly observed in all samples. Diffraction lines for Ru phases (either metallic or oxidized) are not observed in the diffractograms of the fresh samples nor on the diffractograms of the reduced samples (not shown). The lack of diffraction lines, ascribed to the presence of Ru crystalline phases, suggests that Ru particles remain well dispersed on the TiO_2 support and that Ru particle size remains below 4-5 nm. Faint reflections lines ascribed to the presence of TiB_2 can be observed in the diffractogram for the catalyst with the highest amount of B, namely 2B-Ru/TiO_2.

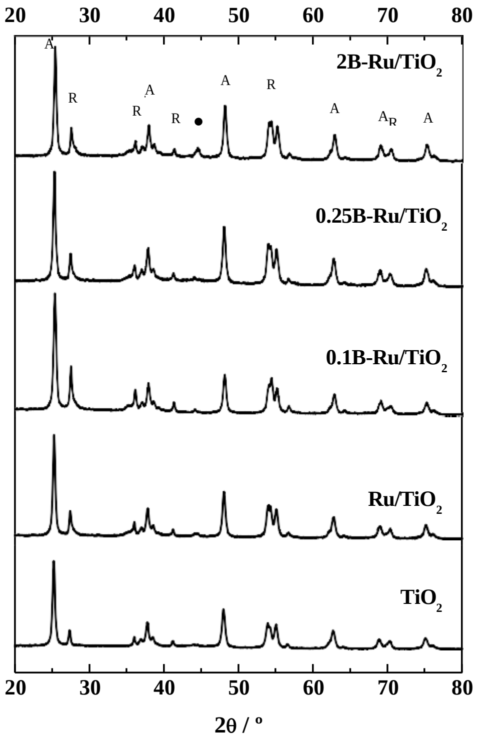

Fig. S1 X-ray diffractograms for the catalysts under study. The diffractogram for TiO_2 is provided for comparison. The characteristic reflection lines for the anatase and rutile phases of TiO_2 are denoted with the letters A and R, respectively. ● is for TiB_2 pdf 01-075-0967

Hydrogen temperature-programmed reduction (H_2-TPR) analyses were carried out with Micrometrics instrument in a U-shaped quartz reactor. Prior to the reduction experiment, the sample (15 mg) was flushed with a He stream at 373 K for 30 min and then cooled down to room temperature. TPR profiles were obtained by heating the sample under a 10 % H_2/Ar flow (50 mL min^{-1}) from 303 to 1173 K (10 K min^{-1}). The TPR profiles for Ru/TiO_2 and 0.25B-Ru/TiO_2 are very similar, exhibiting a main hydrogen consumption peak at approximately 400 K with a shoulder at 450 K. However, the addition of higher amounts of B to Ru/TiO_2 results in a shift of the H_2 consumption profiles towards higher temperatures, exhibiting peak maxima at 453 K. This observation suggests the development of an interaction between Ru and B atoms. Note in passing that all catalysts are completely reduced at 523 K. A similar behavior, namely a shift towards higher reduction temperatures upon B promotion has been reported for Co/Al_2O_3 catalysts.[1] Thus, the results suggest that H_2 dissociation takes place at the same sites for B adsorption, although further studies are needed to confirm this conclusion.

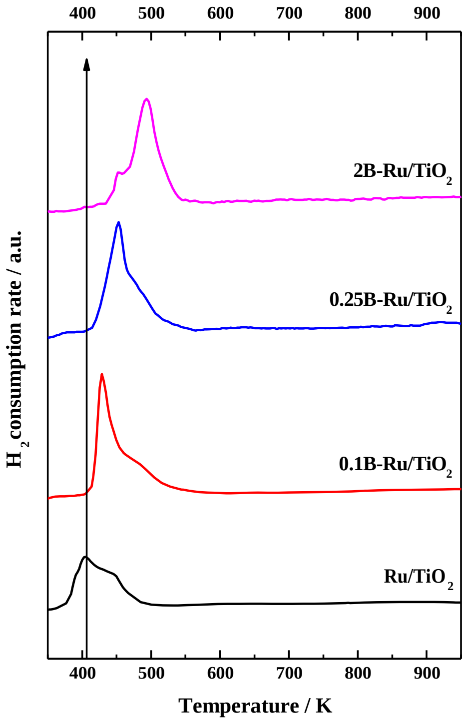

Fig. S2 Hydrogen consumption profiles as a function of temperature for the catalysts with (top) and without B doping (bottom).

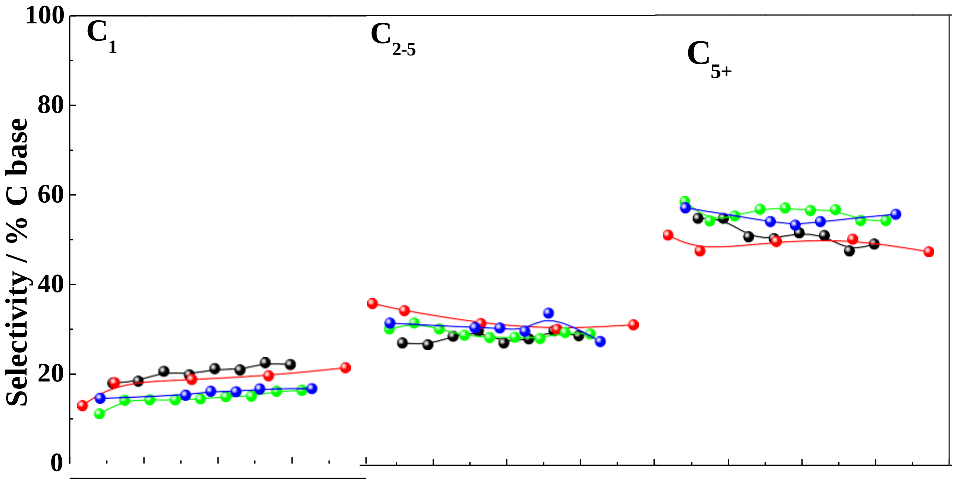

Fig. S3 Evolution of the selectivity towards C_1 (left panel), C_{2-4} (middle panel) and C_5+ (right panel) fractions as a function of time-on-stream for Ru/TiO_2 (black lines), 0.1B-Ru/TiO_2 (red lines), 0.25B-Ru/TiO_2 (green lines) and 2B-Ru/TiO_2 (blue lines). Lines are provided as a guide to the eye.

The relative atomic abundances of B to Ru and Ru to Ti are provided in Table S1.

Table S1. Relative surface abundance of selected elements as derived from XPS data.

Sample	B/Ru at/at	Ru/Ti at/at
0.1B-Ru/TiO_2	0.50	0.09
0.25B-Ru/TiO_2	0.75	0.07
1B-Ru/TiO_2	2.60	0.07
2B-Ru/TiO_2	4.90	0.10

S2. Additional computational details

The separate adsorption energies of *C, *B and *CO in Figure 5 were calculated according to the following reactions:

$$* + C_{(g)} \rightarrow *C \qquad (0)$$

$$* + B_{(g)} \rightarrow *B \qquad (0)$$

$$* + CO_{(g)} \rightarrow *CO \qquad (0)$$

We have included in Tables S2 and S3 the counts used to estimate the generalized coordination numbers of all sites in Figure 4 in the main text and their adsorption energies of *B, *C and *CO.

Table S2. Adsorption sites for *B and *C adsorption on Ru(109).

site location	*CN*	ΔE_B	ΔE_C
hollow @ square step	(2×7 + 6×9 + 2×10 + 8×12) / 26 = 7.07	-7.140	-7.773
hollow @ triangular step	(2×7 + 8×9 + 2×11 + 9×12) / 31 = 6.97	-6.732	-7.296
hcp @ 0001	(6×9 + 3×10 + 7×12) / 23 = 7.30	-6.111	-7.313
hcp @ 0001	(2×7 + 7×9 + 7×12) / 23 = 7.00	-6.246	-7.486
hcp @ 0001	(2×7 + 5×9 + 2×11 + 5×12) / 23 = 6.13	-6.075	-7.301
hcp @ 0001	(2×7 + 4×9 + 2×10 + 5×12) / 23 = 5.65	-6.163	-7.507

Table S3. Adsorption sites for *CO adsorption on Ru(109).

site location	*CN*	ΔE_{CO}
top @ square step	(2×7 + 2×9 + 1×10 + 2×12)/12 = 5.50	-1.927
top @ triangular step	(2×7 + 2×9 + 2×11 + 1×12)/12 = 5.50	-1.853
top @ 0001	(6×9 + 3×12)/12 = 7.50	-1.832
top @ 0001	(2×7 + 4×9 + 3×12)/12 = 7.17	-1.748
top @ 0001	(2×7 + 4×9 + 3×12)/12 = 7.17	-1.789

In Figure S4 we provide several graphical examples of the methodology used in Tables S2 and S3 to assess the generalized coordination numbers on Ru(109).

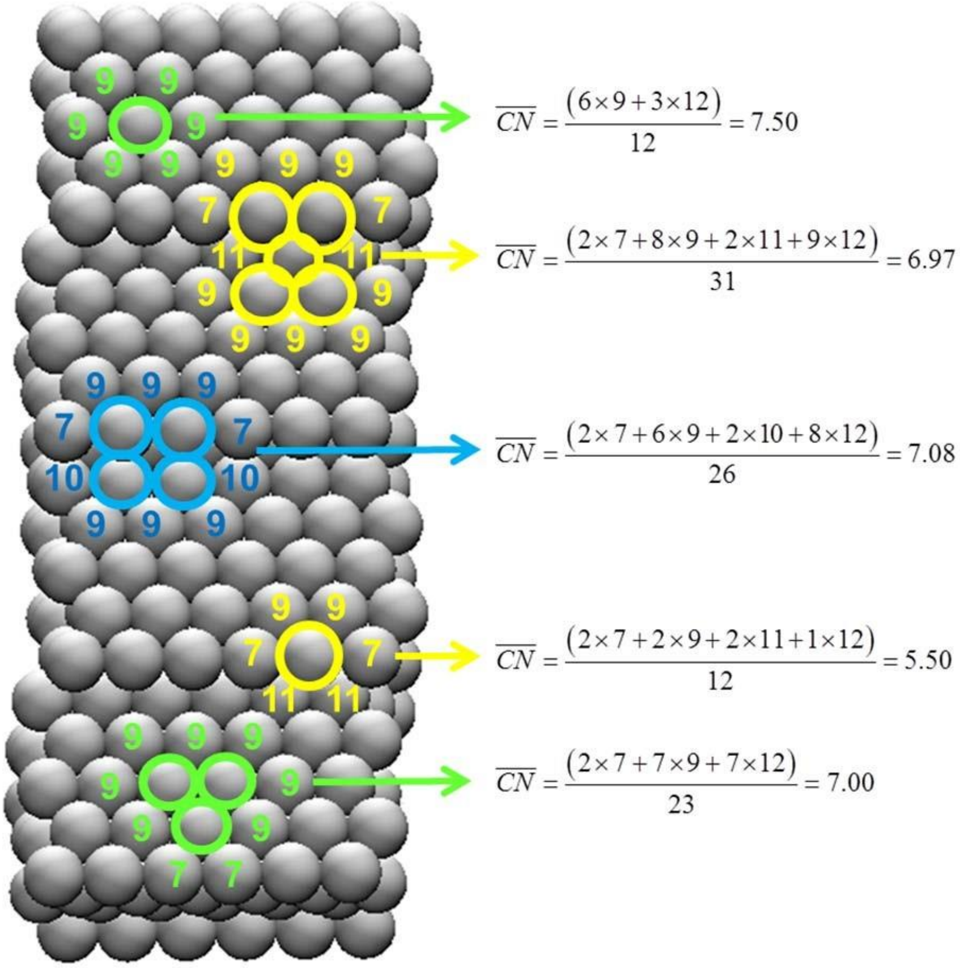

Figure S4. Graphical examples of the assessment of generalized coordination numbers on Ru(109). In all cases, the coordination of the nearest neighbors is provided, except for those with cn = 12, which are in the subsurface layers.

Table S2. Adsorption sites for *B and *C adsorption on Ru(109).

site location	$\overline{CN}$	ΔE_B	ΔE_C
hollow @ square step	(2×7 + 6×9 + 2×10 + 8×12) / 26 = 7.07	-7.140	-7.773
hollow @ triangular step	(2×7 + 8×9 + 2×11 + 9×12) / 31 = 6.97	-6.732	-7.296
hcp @ 0001	(6×9 + 3×10 + 7×12) / 23 = 7.30	-6.111	-7.313
hcp @ 0001	(2×7 + 7×9 + 7×12) / 23 = 7.00	-6.246	-7.486
hcp @ 0001	(2×7 + 5×9 + 2×11 + 5×12) / 23 = 6.13	-6.075	-7.301
hcp @ 0001	(2×7 + 4×9 + 2×10 + 5×12) / 23 = 5.65	-6.163	-7.507

Table S3. Adsorption sites for *CO adsorption on Ru(109).

site location	*CN*	ΔE_{CO}
top @ square step	(2×7 + 2×9 + 1×10 + 2×12)/12 = 5.50	-1.927
top @ triangular step	(2×7 + 2×9 + 2×11 + 1×12)/12 = 5.50	-1.853
top @ 0001	(6×9 + 3×12)/12 = 7.50	-1.832
top @ 0001	(2×7 + 4×9 + 3×12)/12 = 7.17	-1.748
top @ 0001	(2×7 + 4×9 + 3×12)/12 = 7.17	-1.789

References

[1] K. F. Tan, J. Chang, A. Borgna, M. Saeys, J. Catal. 2011, 280, 50-59.